Science & Technology Development Journal – Engineering and Technology 2025, 8(3):2612-2622

Open Access Full Text Article

Research Article

Bending collapse behaviour of thin-walled high strength steel under static and dynamic impact loading

Hai Tran[1,*], Leonardo Gunawan[2], Sigit. P. Santosa[2], Annisa Jusuf[2], Tatacipta Dirgantara[2], Tuan Le-dinh[1], Tao Tran-van[1]

ABSTRACT

This paper studies a type of collision that is dangerous to crash worthiness structures and of great interest, the side impact collision. In this study, the bending collapse behavior of thin-walled high strength steel material under side impact was investigated numerically and experimentally. For both static and dynamic side impact loads, the bending collapse behavior such as load carrying capacity, deformation characteristics, and energy absorbing capability were carried out by using three-point bending model. Based on the numerical simulation, those bending collapse responses were predicted and after that this simulation was validated by experimental analysis in cases of static and dynamic bending test. There were two bending specimens for each dynamic and static impacts performed in the experiment. First, the numerical and experimental results showed that the total energy absorption of high strength steel beam in dynamic bending was higher than those in static bending load. Second, the comparison between numerical and experiment pointed out a good agreement with respect to the bending crush force-deformation characteristics at small rotation of beams. Moreover, the effects of geometrical at the corners, mesh size, friction coefficient on the bending resistance behavior is also analyzed and carried out in this study. Namely, in the same bending load, with corner radius, the localized deformation can easily be created than those in right angle corner of beam. The friction coefficient will not affect peak force. The different peak force is predicted as 1% when the coefficicent increases from 0 to 0.2. The empirical formula was founded to be able to predict the ultimate bending moment crush under dynamic bending loads within the effect of strain rates and impact velocities. The good comparison results in terms of dynamic ultimate bending moment between numerical simulation, empirical prediction and experiment indicated the reliability in calculation for dynamic ultimate bending moment under dynamic bending conditions.

Key words: Bending collapse, Crashworthiness, Crush resistance response, High strength steel, Energy absorption beam

[1]*Ho Chi Minh City University of Technology (HCMUT), VNU-HCM, Vietnam*

[2]*Bandung Institute of Technology, Indonesia*

Correspondence

Hai Tran, Ho Chi Minh City University of Technology (HCMUT), VNU-HCM, Vietnam

Email: haitran@hcmut.edu.vn

History

- Received: 20-09-2023
- Revised: 09-11-2024
- Accepted: 05-08-2025
- Published Online: 29-09-2025

DOI :

https://doi.org/10.32508/stdjet.v8i3.1207

INTRODUCTION

Thin-walled structures have been used commonly as energy absorbing components in transportation vehicles with many advantages to reduce the injuries or protect the passengers during collision events. Accident data showed that bending collapse of structures in side impact case was one of the main reasons that cause the injuries to passengers because of limited space between the occupants and structural members. Consequently, determining the deformation and ultimate strength as well as energy absorption of thin-walled structures under bending collapse became importantly to figure out the bending resistance of their components. Several studies investigated the energy absorbing capability of crashworthy structures under axial impact loading [1–3] while a few researchers concentrated on bending resistance behavior of thin-walled beams [4–6]. Santosa SP. and Wierzbicki T.[7] explored in bending collapse behavior of thin-walled prismatic columns in static situation by determining the effect of ultralight metal filler. Their analytical and numerical results contributed the advantages of low-density core filler in increasing the bending resistance compared to empty columns. Santosa SP., et al.[8] studied the bending resistance behavior of thin-walled beam with aluminum foam-filled section through experimental and numerical analyses. They showed that the aluminum foam filler provided a higher bending resistance and changed from single stationary fold to multiple propagating folds. Soo H., et al.[9] focused on the crush behavior of thin-walled prismatic columns under combined bending and compression. Liu Y., et al.[10,11] conducted bending collapse study of thin-walled circular tubes and its computational application. In their paper, they described the relationship between the bending moment and the rotation angle of circular tubes, and

Cite this article : Tran H, Gunawan L, Santosa S P, Jusuf A, Dirgantara T, Le-dinh T, Tran-van T. **Bending collapse behaviour of thin-walled high strength steel under static and dynamic impact loading**. *Sci. Tech. Dev. J. – Engineering and Technology* 2025; 8(3):2612-2622.

they also showed those absorbed energies. Guo L., et al.[12,13] developed the bending resistance of traditional single wall circular tubes by changing into double walls cylindrical tubes with aluminum foam core. With new composite material, they concluded that the specific energy absorption efficiency was much higher than the old one in terms of static bending.

Based on the above studies, it is significant to get a comprehensive analysis and evaluation for bending resistance of thin-walled beams. Most of the above works just focus on bending behaviour under quasi-static loading, and they have not used high strength material such as high strength steel which is used widely in modern vehicles for side impact problems. Therefore, the objective of the present work is to study bending response of thin-walled high strength steel beams through both of dynamic and static bending load conditions. Static experiments are conducted by traditional three-point bending while dynamic experiment is carried out in detail by drop bending tests. The numerical analysis is executed by using finite element explicit code LS-DYNA and compared to experimental results. The results are also compared in terms of the effects of corner radius, size and element mesh density, friction coefficient on bending crush resistance of beam for static and dynamic bending collapse conditions. More importantly, the empirical prediction formula on the ultimate bending moment is proposed under dynamic bending load conditions within the effect of strain rates.

THEORETICAL ANALYSIS

Theoretical analysis was based on the assumptions that the walls of a section of empty square beam deformed along the concentrated yield lines only. In particular, the central portion of empty square beam was known as a main location of deformation formed by bending loads. Furthermore, this location was also where the plastic deformation energy dissipated through the traveling hinge lines, compressible and extensible flanges. A simplified model of bending collapse of empty beam was shown in Figure 1.

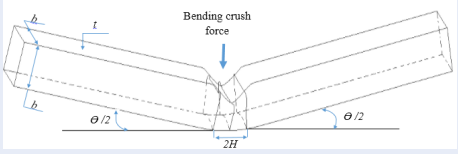

Figure 1: A typical local deformation of empty beam under bending loads

Bending crush predictions

As shown in Figure 1, plastic deformation occurs between two un-deformed beam segments. The boundaries are clearly defined by the stationary hinge lines and half of the distance between those hinge lines is called half folding length (H). By considering the parameters of empty beam which has cross-section b x b, thickness t, undergo bending rotation Θ, haft folding length is obtained[7,8]

$$H = 1.276 b^{\frac{2}{3}} t^{\frac{1}{3}} \tag{1}$$

The characteristic of bending moment-rotation was derived by Wierzbicki and Santosa[7,8] for analytical solution:

$$M(\theta) = 2P_m b(0.576 + \frac{1}{2\sqrt{\theta}}) \tag{2}$$

where

$$P_m = 2.76\sigma_0 b^{\frac{1}{3}} t^{\frac{5}{3}} \tag{3}$$

And the equivalent flow stress σ_0 is calculated[14]

$$\sigma_0 = \sqrt[3]{\frac{2\sigma_y \sigma_u^2}{(n+1)^2 (n+2)}} \tag{4}$$

with σ_o is dynamic flow stress, σ_y and σ_u are dynamic yield strength and ultimate strength, n is strain hardening exponent.

The approximation for bending ultimate moment of empty beam was given[8]

$$M_u^0 = 4.65\sigma_0 b^{\frac{5}{3}} t^{\frac{4}{3}} \tag{5}$$

The critical bending rotation θ_c for local sectional collapse is obtained by substituting equation (2) in to equation (5)[8]

$$\theta_c = \frac{1}{4}\left[\frac{1}{0.8\left(\frac{b}{t}\right)^{\frac{1}{3}} - 0.576}\right]^2 \tag{6}$$

Hence, the moment-rotation response of empty beam is presented as follow by Santosa[8]

$$M_u^0(\theta) = \begin{cases} \frac{5}{3} t^{\frac{4}{3}} & (0 \le \theta \le \theta_c) \\ 4.65\sigma_0 b^{\frac{5}{3}} & \\ 2P_m b(0.567 + \frac{1}{2\sqrt{\theta}}) & (\theta \ge \theta_0) \end{cases} \tag{7}$$

Material characterization

In bending collapse condition for side impact, the structural components not only have to undergo a high force during crash event but also must withstand a large deformation especially under dynamic bending loads. The response of square beam to dynamic bending loads is that produce large plastic deformation. Otherwise, the energy absorption capability of systems in large deformation is higher than small deformation because of plastic strain [15]. Therefore, in analysis, the elastic strain can be ignored, and material's property stress-strain curves are idealized as a rigid power hardening material as equation (8)

$$\begin{cases} \leq \sigma_y & for \quad \varepsilon = 0 \\ = \sigma_y + K\varepsilon^n & for \quad 0 < \varepsilon < \varepsilon_f \end{cases} \tag{8}$$

with the term Kdenotes hardening modulus and n is strain hardening exponent/power law exponent of material as previous explanation. $\sigma_y$was mentioned in Eq. (4), ε and ε_f are strain and strain at fracture point of material.

Besides, the effect strain rate in bending collapse was considered in some researches of Jones [16] and Rawling [17]. According to these authors, for material sensitivity such as high strength steel, the dynamic yield stress will increase as the strain rate increases. This characteristic is demonstrated in Figure 2.

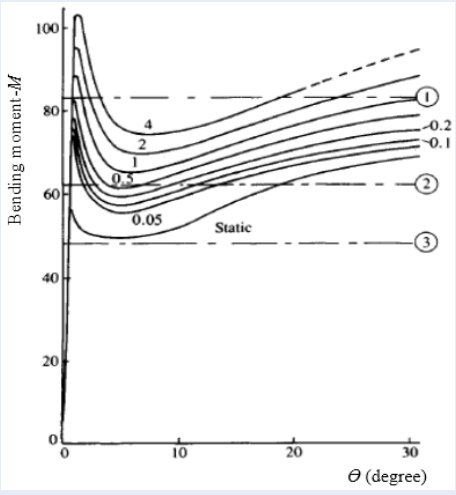

Figure 2: Comparison of dynamic bending moment-rotation curves. 1): $\dot{\theta} = 4^0$/ms ($\dot{\varepsilon} \cong 12s^{-1}$); 2): 1): $\dot{\theta} = 0.05^0$/ms ($\dot{\varepsilon} \cong 0.15s^{-1}$). Numbers on curves are values of 1): $\dot{\theta} = {}^0$/ms [16]

NUMERICAL MODELING AND SIMULATIONS

For simulating, the bending resistance characteristics of thin-walled high strength beams subjected to static and dynamic bending load were studied by using a commercial finite element explicit code LS-DYNA. The beams wall was modeled with Belytschko - Tsay 4 – node thin shell element while the impactor was modeled as a rigid cylinder.

Geometrical modeling

The thin-walled empty square beam with cross sectional geometry 40 × 40 × t mm and length L = 470 mm is considered in the analysis. The punch is modeled by using a finite rigid cylinder with radius r = 25 mm and length l = 124 mm. Two supports are also modeled as a stationary rigid cylinder with the same length and radius with the punch and they are spaced d = 370 mm apart. The contacts surface-to-surface between rigid cylinder and wall was utilized in this simulation.

Besides, for static bending collapse, the distance between the punch and wall is set small enough to make the beam unaffected by inertia load of impactor. The velocity boundary condition is applied on the rigid punch. It is shown in Figure 3(a). The velocity gradient is from 0 m/s to 0.1 m/s during the first 50 milliseconds (static loading) and then this velocity is held at a constant value. Figure 3 (b) presents dynamic bending simulation; the initial velocity is applied on the impactor and it is not constant during the collision.

Corner modeling

An actual beam always has finite corner radius and the thickness at the corner is not same compared to the thickness of the walls of the square beam. Therefore, the effect of geometrical imperfection was critical to determine the bending collapse response of the thin-walled high strength steel beams, thus detail modeling at the corners of the beams needed to evaluate their influences. Considering the influence of 4 corners of square beam is significant to get reliable result in numerical simulation. One beam with bending radius at the corners is modeled as Figure 4. In this study, the bending radius (r) at 4 corners is chosen such that this radius equals to bending radius of an actual beam. The thickness at the corners is from 1.2 mm to 1.5 mm.

Mesh density strategy

As mentioned in section 2, the bending crush was expected to occur at the central portion of the beams due to localized nature of deformation. Therefore,

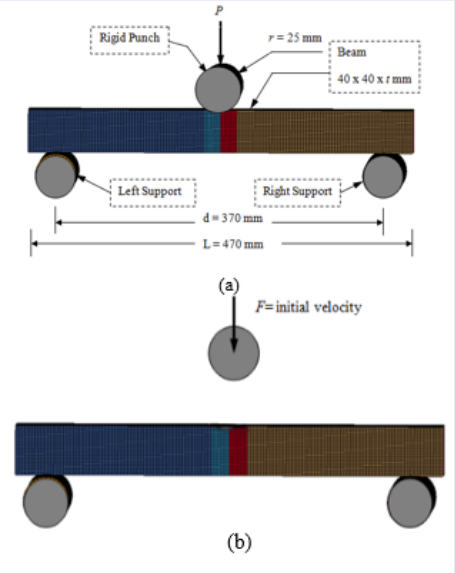

Figure 3: Finite element model of (a) static and (b) dynamic bending collapse

Figure 4: Square beam with radii corner r in simulation

the central segment of beam was modeled with finite mesh size of element 2.5 × 2.5 mm while the mesh size for un-deformed segment was 2.5 × 3.5 mm as seen in Figure 5. Because the length of bending crush region can be obtained by using equation (1), thus the localized length need is greater than the folding length ($2H$). For the greatest thickness of the beams (t=1.5 mm), the localized length l_c was predicted to be greater than 40 mm. In this numerical simulation, l_c was taken as 100 mm. Otherwise, once again, the mesh size of element at the corner of square beam needs to be considered carefully based on the convergence test and acceptable processing time.

EXPERIMENTAL STUDY

Specimen preparation

Four thin-walled beams were used in the experiments. Each beam was formed by a thin sheet with four bending lines at four corners and a welding line at the middle of the bottom wall. Because welding line led to inconsistency in thickness and material's property of

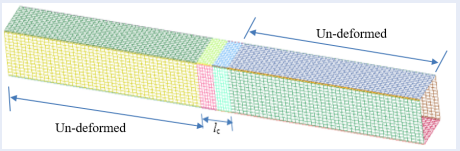

Figure 5: Different mesh size at bending crush length and un-deformed segments

beam, the placement of that welding line was taken to have little effect on the bending behavior of beam during experimental process. Square cross-sectional geometry, thickness and the length of thin-walled beam was chosen respectively b = 40 mm, t =1.5 mm, L = 470 mm, shown in Figure 6. Due to manufacturing process, there are variations on the geometrical measurement of the beams, thus it is needed to measure correctly parameters of models, as presented in Table 1.

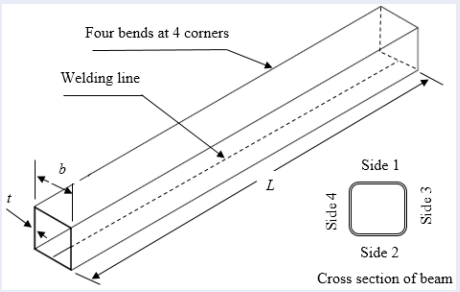

Figure 6: Schematic drawing of high strength steel square beam specimen

In Table 1, there were 2 beams for static and 2 beams for dynamic bending test.

As previously discussed, in numerical simulation, the stress-strain curves of material need to define. The mechanical properties of thin-walled beam stress-strain curves characteristics were obtained from varying tensile tests in Computational Solid Mechanics and Design Laboratory – Korea Advance Institute of Science and Technology (CSMD laboratory–KAIST). Fifteen tensile test samples were taken from same material with the thin-walled beams. Details of these samples can be founded in Figure 7.

The test was conducted to carry out the material's properties in quasi-static and dynamic with various strain rates and these are listed in Table 2 and Figure 8

Experiment set-up

Table 1: Geometrical details of high strength steel beams for bending experiments

Specimen	Beam thickness t (mm)	Outer width b (mm)			
		Side 1	Side 2	Side 3	Side 4
S-U255	1.5	40.5	40.5	38.7	39.5
S-U256	1.5	40.3	40.3	39.6	39.8
D-U255	1.5	40.2	40.2	39.2	39.0
D-U256	1.5	40.2	40.5	39.0	38.7

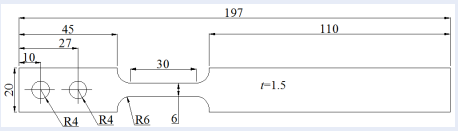

Figure 7: Specimen preparation for tensile testing

Table 2: Material properties of high strength steel CR-CHSP420Y

Material	High strength steel-CR-CHSP420Y
Young's modulus, E (MPa)	2×10^5
Yield stress, σ_y (MPa)	420
Density (kg/mm^3)	7.83×10^{-6}
Poisson's ratio, ν	0.3
Ultimate strength, σ_u (MPa)	570
Power law exponent, n	0.26

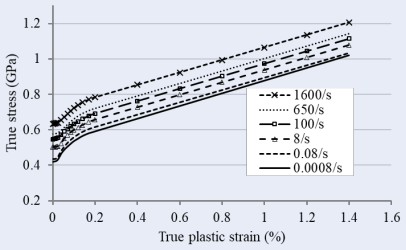

Figure 8: True stress–True plastic strain curves of CR-CHSP420Y at various strain rates

Quasi- static bending test

Two thin-walled beams were tested under quasi-static bending load with three-point bending model on HT-2101 Series Universal Testing Machine at Metal Industry Development Center (MIDC), Bandung, Indonesia. The 0.03 mm/s impact velocity was chosen in this experiment. Two supports were spaced d = 370 mm apart and radius of punch and two supports were r = 25 mm, as shown in Figure 9.

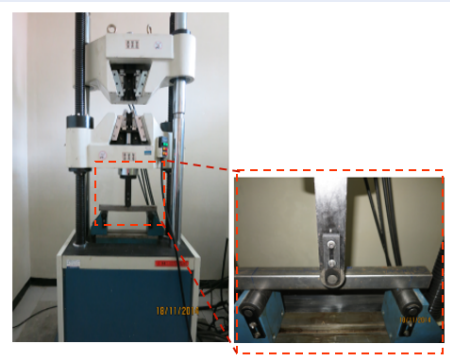

Figure 9: Set-up three-point bending for static test

Dynamic bending test

By using the similar two high strength steel beams in quasi-static, the dynamic bending tests were studied with drop test machine in Lightweight Structure Lab, Institut Teknologi Bandung, Indonesia. The impact mass was approximately 50 kg and the height of impactor was 1500 mm. Therefore, kinetic energy was 735 Joule. The experiment set-up is shown schematically in Figure 10.

RESULT COMPARISON AND DISCUSSIONS

Effect of frictions

Friction is an important factor which affects the bending resistance results. In terms of frictionless contact

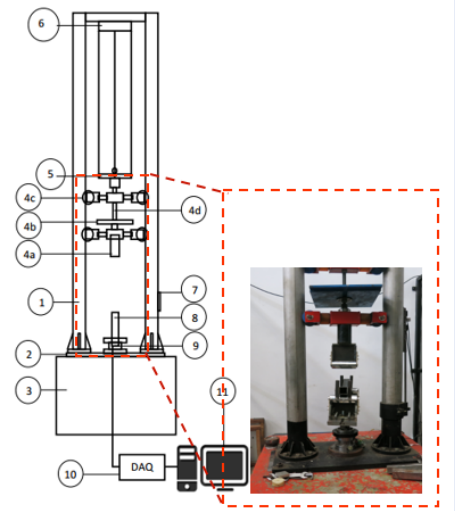

Figure 10: Schematic showing the dropped weight impact machine for dynamic bending test at Institut Teknologi Bandung, Indonesia

conditions, the lower bending crush force response after reaching the peak force value will be obtained in simulation compared to experimental results. It is shown in Figure 11. In the experiments, no lubrication was used so that there must have been significant frictional force on the punch- beam interface. The theoretical analysis for frictional force was explored in [7,8]

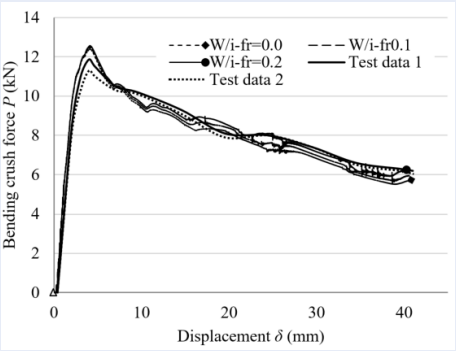

Figure 11: Static bending crush force-displacement response for various friction coefficient 0, 0.1 and 0.2

In reality, the friction coefficient will not affect peak force. The different peak force is predicted as 1% when the coefficicent increases from 0 to 0.2. However, consider the whole of bending collapse process, the higher friction coefficient gives higher bending crush force after local sectional collapse occurs at relatively small roatation angle. It is demonstrated in Figure 11. By observing the final results, with 0.2 friction coefficient in contact, bending crush force in numerical is closer to experimental result than those with 0 and 0.1 friction coefficient.

Effect of corner modeling

The higher peak force on the perfect beam can be explained by observing the initial deformation of beam. Two types of deformation exhibit, rolling deformation and the initial buckling on the vertical edges require very high force. In addition, the actual beam has finite corner radius so that the initial rolling deformation requires lower load than the perfect beam with sharp corners. It is presented in Figure 12

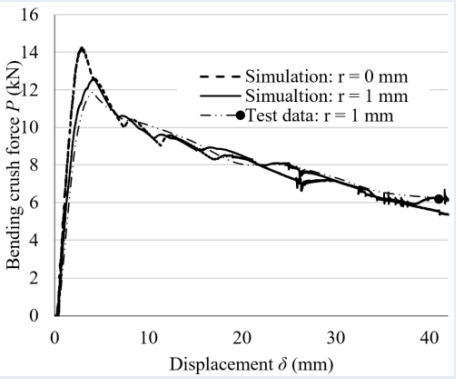

Figure 12: Static bending crush- displacement response with different corner radius values

The expression for this difference comes from the effect of corner radius of beams. In this study, the thin-walled beams are made from high strength steel sheet which is bent at 4 corners with radius r =1 mm. Therefore, evaluating the effect of corner radius is very important in order to obtain the bending crush force in simulation analysis. By observing Figure 13, it can be seen that in the same bending load, with corner radius, the localized deformation can easily be created than those in right angle corner of beam.

Besides that, the erroneousness in theroretical and numerical to experiment are from the different thickness at 4 corners of beam. It is indicated in Figure 14

Static and dynamic bending crush force resistance

Figure 15 presents that load-carrying capacity of thin-walled high strength steel beams under dynamic

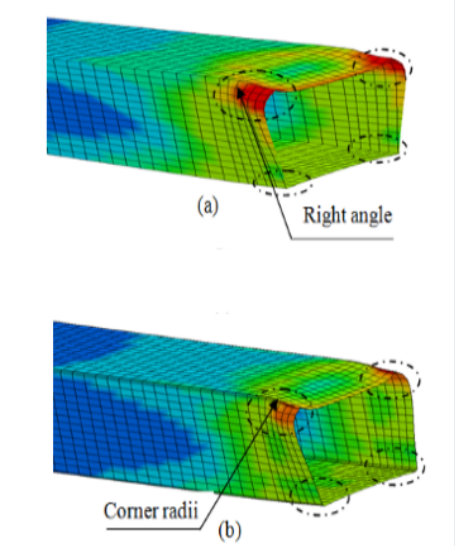

Figure 13: Bending collapse model (a) Right angle corner and (b) Corner radius-r = 1 mm

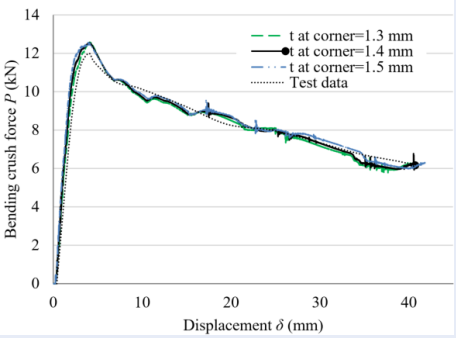

Figure 14: Effect of thickness at the corner on static bending crush force

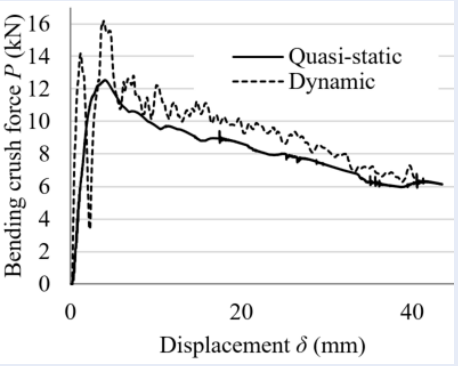

Figure 15: Static and dynamic bending crush force comparison in numerical simulation

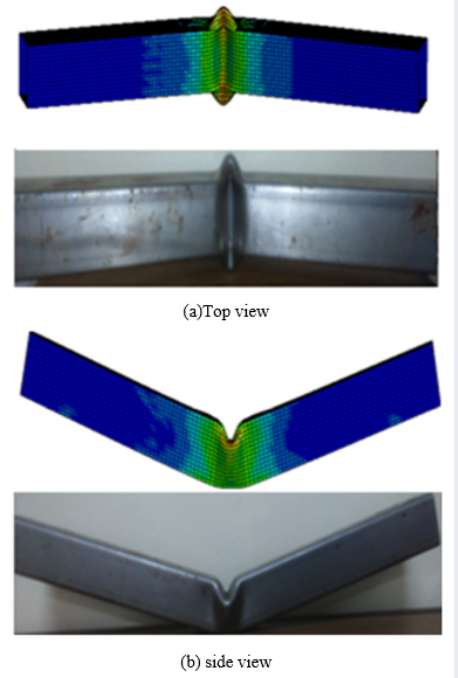

Figure 16: Static deformation model of empty beam in numerical simulation and experiment

bending is higher than those in quasi-static bending. After undergoing the critical load (peak bending crush force), the bearing load capacity of beam declined in the same value for both static and dynamic cases. Besides, Figure 15 also shows that the higher bending crush resistance of beam under dynamic bending compared to static bending conditions. By observation, Figure 16 shows a very good agreement in deforming characteristics of square tube under bending load between simulation and experiment.

Static and dynamic ultimate bending moment resistance

In numerical analysis, the bending crush moment can be calculated from bending crush force. It is derived from [14]

$$M(\theta) = \frac{P(\theta)L}{4} \tag{9}$$

where $P(\theta)$ is a punch force at rotation angle (θ)

The small value of rotation angle of beam can be approximated as follows [14]

$$\theta = arctan\left(\frac{2\delta}{L}\right) \quad (10)$$

where $\delta(\theta)$ is a total displacement at central of beam at rotation angle

By applying equation (9), the bending crush moment of beam under static and dynamic bending conditions are drawn in Figure 17

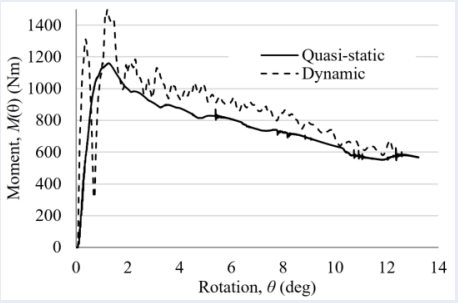

Figure 17: Static and dynamic bending crush moment in numerical simulation

Total energy absorption comparison in static and dynamic bending

The total energy absorption EA can be obtained by integrating the bending moment-rotation curve [14]

$$EA = \int_0^{\theta_{max}} \int_0^{\theta_c} M(\theta)d(\theta) \int_{\theta_c}^{\theta_{max}} M(\theta)d(\theta) M(\theta)d(\theta) \quad (11)$$

or in numerical EA can be replaced by

$$EA = \sum_{i=1}^{n} (M_{\theta(i)} + M_{\theta(i+1)}) \left(\frac{\theta_{(i+1)} - \theta_{(i)}}{2}\right) \quad (12)$$

By applying equation (12), total energy absorption of thin-walled beams subjected to dynamic and static bending are compared and shown in Figure 18

Figure 18 shows that the energy absorption capability of beam under dynamic bending is greater than those in static bending. In other words, the higher bending crush resistance of beam in dynamic impact conditions is due to larger plastic deformation

Empirical predictions on bending crush resistance

As we known that the strain rate affects the bending resistance behavior of thin-walled beam under high velocity impact conditions due to the change of flow stress in strain rate sensitivity material. The ultimate bending moment was introduced in equation (5) is

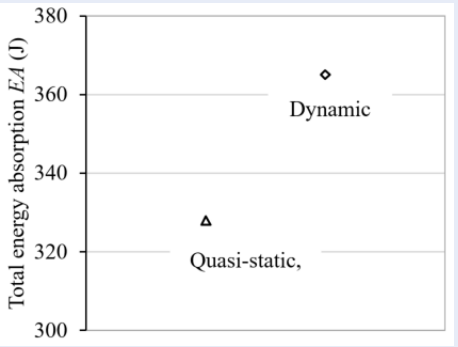

Figure 18: Total energy absorption comparison between static and dynamic bending

only applicable for static bending case and it is not suitable to use in dynamic bending instance under high impact velocity. Therefore, the empirical prediction on bending crush resistance becomes significantly to find a general formula for dynamic bending loads. The bending crush forces and ultimate bending moment under various high velocities in finite element analysis are shown in Figure 19 and Table 3 respectively.

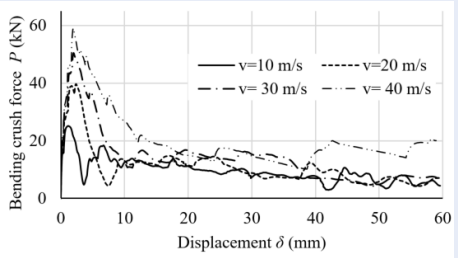

Figure 19: Dynamic bending crush force with various impact velocities

By performing the dynamic ultimate bending moment values M_u^d in to a diagram, it can be seen that these values are distributed according to the power function of variable impact velocity or strain rate. It is shown in Figure 20

Therefore, for high impact velocity within the effect of strain rate, equation (5) is developed to be able to predict dynamic ultimate bending moment, as below

$$M_u^d = 0.945 M_u^0 \varepsilon^{0.1219} \quad (13)$$

where ε (1/s) is strain rate of material.

To validate empirical formula on ultimate bending moment (Eq. 13), two drop bending experiments

Table 3: Ultimate bending moment in static and dynamic impact loadings

Bending conditions	Impact velocity v (m/s)	Strain rate (ε) (s^{-1})	Ultimate bending Moment M_u (N.m)
Quasi-static	0.1	0.08	1160
Dynamic D_{01}	10	8	2280
Dynamic D_{02}	20	100	3670
Dynamic D_{03}	30	650	4670
Dynamic D_{04}	40	1600	5470

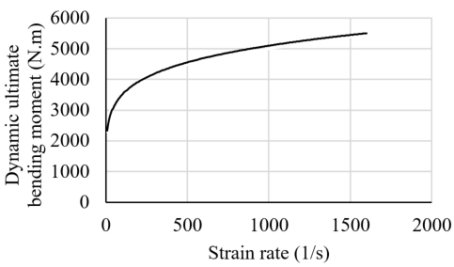

Figure 20: Power distribution of dynamic ultimate bending moment – M_u^d

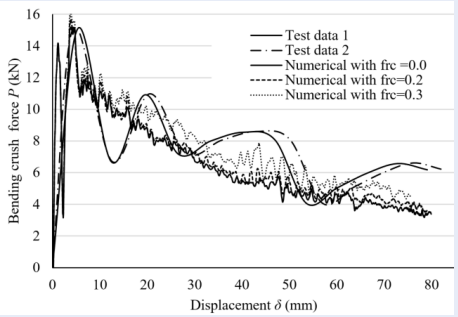

Figure 21: Numerical and experimental comparison on dynamic bending crush forces

with similar specimens were conducted and the results showed the similar bending crush forces versus displacements in two tests. Foremost, by comparing the results, peak forces in numerical simulation were close to those in experiments. It is depicted in Figure 21. In addition, the effect of friction coefficient is also presented on the behaviors of beams after reaching maximum load. The peak forces in numerical analysis do not change for different friction coefficients$\mu = 0,\ 0.2,\ 0.3$. However, if consider the entire of bending collapse, higher friction coefficient gives higher bending crush force. In most of the cases, there is good matching between numerical and experimental results. In addition, Figure 22 displays the deformation pattern of thin-walled high strength steel beams under dynamic bending.

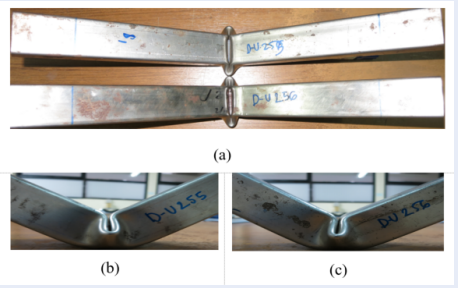

Figure 22: Deformation pattern of thin-walled high strength steel beams under dynamic bending: top view, (b) and (c) side view

Otherwise, the comparisons on ultimate bending moment between numerical analysis, experiment and empirical prediction are figured out in Figure 23

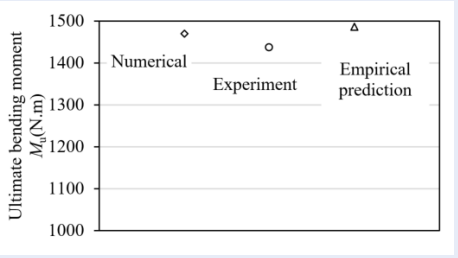

Figure 23: Compared dynamic ultimate bending moment by using numerical, experimental and empirical prediction methods

CONCLUSION

In this paper, the bending collapse resistance of thin-walled high strength steel beams was addressed by using finite element and experimental methods. The comparisons with the effect of friction between numerical and experimental analyses show that a good agreement in terms of bending crush force was founded with $\mu = 0.2$ friction coefficient for static

bending conditions. In addition, the beams within corner radius r = 1 mm in numerical simulation also show a good result of bending crush force compared to experiment, and it can be seen that the thickness at each corner affect bending resistance of beam. Otherwise, under dynamic bending loads, bending crush force, ultimate bending moment and total energy absorption are higher than those in static bending event. Therefore, it is concluded that the bending crush behavior of beam can be improved in terms of undergoing a dynamic bending load instead of a static bending. In other words, design influence by using dynamic bending behavior is rather than static bending to avoid over design with static resistance. Furthermore, empirical formula predicted very well on dynamic ultimate bending moment under dynamic loads. It was shown in Fig. 23. By employing dynamic drop test, the results in empirical prediction and numerical finite element were validated and showed a very good matching for dynamic ultimate bending moment (M_u^d)at various impact velocities and strain rate (difference <5%).

ACKNOWLEDGEMENTS

We gratefully acknowledge AUN/SEED-Net (Southeast Asia Engineering Education Development Network) for supplying financial, Lightweight Structure Research Group, ITB. The authors would like to thank to the Computational Solid Mechanics and Design Laboratory–Korea Advance Institute of Science and Technology (CSMD Laboratory–KAIST) for finding the properties of material in static and dynamic conditions. We also express our gratitude to Livemore Software Technology Corporation–LSTC for providing education licenses of program LS-DYNA. Finally, thank are also due to my colleague in Lightweight Structure Lab - Mr. Agustinus Dimas for helping to do tensile test.

CONFLICT OF INTEREST

We declare that there is no conflict of whatsoever involved in publishing this research.

AUTHORS' CONTRIBUTIONS

Dr. Hai Tran carried out the experiment, collecting, analyzing experimental data, and writing the manuscript. Prof. Tuan Le-dinh and Msc. Tao. Tranvan shared with me their relevant knowledge. Prof. Leonardo Gunawan, Dr. Sigit. P. Santosa, Dr. Annisa Jusuf, and Prof. Tatacipta Dirgantara guided me throughout my research.

REFERENCES

1. Wierzbicki T, Abramowicz W. On the crushing mechanics of thin-walled structures. Journal of Applied Mechanics. 1983;50:727–39.
2. Abramowic W, Jones N. Dynamic axial crushing of square tubes. Int J Impact Eng. 1984;2(2):179–208.
3. Jusuf A, Dirgantara T, Gunawan L, Putra IS. Crashworthiness analysis of multi-cell prismatic structures. Int J Impact Eng. 2015;78:34–50.
4. Kecmand. Bending collapse of rectangular and square section tubes. Int J Mech Sci. 1983;25(9-10):623–36.
5. Wierzbicki T, Recke L, Ambramowicz W, Gholami T, Huang J. Stress profiles in thin-walled prismatic columns to crush loading-II. Bending. Computer and Structures. 1994;51(6):625–641.
6. Park MS, Lee BC. Prediction of bending collapse of thin-walled open section beams. Thin-Walled Struct. 1996;25(3):185–206.
7. Santosa SP, Wierzbicki T. Effect of an ultralight metal filler on the bending collapse behavior of thin-walled prismatic columns. Int J Mechanical Sciences. 1999;41:995–1019.
8. Santosa SP, Banhart J, Wierzbicki T. Experimental and numerical analysis of bending of foam-filled sections. Acta Mechanical. 2001;148:199–213.
9. Soo H, Wierzbicki T. Crung behavior of thin-walled prismatic columns under combined bending and compression. Computers and Struct. 2001;79:1417–1432.
10. Liu Y, Day ML. Bending collapse of thin-walled beams with channel cross-section. Int J Crash. 2006;11(3):251–261.
11. Liu Y, Day ML. Bending collapse of thin-walled circular tubes and computational application. Thin-Walled Struct. 2008;46:442–450.
12. Guo L, Yu J. Dynamic bending response of double cylindrical tubes filled with aluminum foam. Int J Impact Eng. 2011;38:85–94.
13. Li Z, Zheng J, Yu J, Guo L. Crashworthiness of foam-filled thin-walled circular tubes under dynamic bending. Material and Design. 2013;52:1058–1064.
14. Santosa SP. Crashworthiness Analysis of Ultra-Light Metal Structures. Cambridge, MA-02139, USA; 1999.
15. Jusuf A. Crashworthiness Analysis of Multi-cells and double-walled Foam Filled Prismatic Structures. 2012;.
16. Jones N. Structural Impact. and others, editor. Cambridge University Press; 1989.
17. Rawlings B. Energy absorption of dynamically and statically tested mild steel beams under conditions of gross deformation. International Journal of Mechanical Sciences. 1967;p. 633–638.

Tạp chí Phát triển Khoa học và Công nghệ – Kỹ thuật và Công nghệ 2025, 8(3):2612-2622

Open Access Full Text Article

Bài nghiên cứu

Ứng xử hỏng do uốn của kết cấu hộp thép độ cứng cao thành mỏng dưới lực va chạm tĩnh và động

Trần Hải[1,*], L. Gunawan[2], SP. Santosa[2], A. Jusuf[2], T. Dirgantara[2], Lê Đình Tuân[1], Trần Văn Tạo[1]

Use your smartphone to scan this QR code and download this article

TÓM TẮT

Bài báo này nghiên cứu một loại va chạm nguy hiểm đối với các kết cấu chịu va chạm và rất được quan tâm, va chạm tác động bên. Trong nghiên cứu này, đặc tính hư hỏng do uốn của kết cấu thép cường độ cao thành mỏng đã được nghiên cứu bằng phương pháp số và thực nghiệm. Đối với cả hai trường hợp tải trọng uốn tĩnh và động, các đặc tính hư hỏng do uốn như khả năng chịu tải, đặc tính biến dạng và khả năng hấp thụ năng lượng đều được nghiên cứu thực hiện bằng cách sử dụng mô hình uốn ba điểm. Dựa trên mô phỏng số, các phản ứng hư hỏng do uốn này đã được dự đoán và xác nhận bằng phân tích thử nghiệm trong điều kiện uốn tĩnh và động. Có hai mẫu uốn cho mỗi tác động động và tĩnh được thực hiện trong thí nghiệm. Đầu tiên, các kết quả tính toán số và thực nghiệm cho thấy tổng năng lượng hấp thụ của dầm thép cường độ cao khi chịu tải uốn động cao hơn khi chịu tải trọng uốn tĩnh. Hơn nữa, so sánh giữa mô phỏng số và kết quả thực nghiệm cho thấy có sự phù hợp tốt về đặc tính lực uốn - biến dạng khi góc xoay của dầm nhỏ. Hơn nữa, ảnh hưởng của các yếu tố như yếu tố hình học tại các góc, yếu tố về kích thước mắt lưới, yếu tố hệ số ma sát đến ứng xử chịu uốn của kết cấu cũng được phân tích và thực hiện trong nghiên cứu này. Cụ thể, trong cùng một tải uốn, với bán kính góc, biến dạng cục bộ có thể dễ dàng được tạo ra hơn so với biến dạng ở góc vuông của dầm. Hệ số ma sát sẽ không ảnh hưởng đến lực cực đại. Lực cực đại khác nhau được dự đoán là 1% khi hệ số tăng từ 0 đến 0,2. Ngoài ra, công thức thực nghiệm đã được thành lập để có thể giúp dự đoán mômen phá hủy cực đại dưới tác dụng của tải trọng uốn động khi có xét đến ảnh hưởng của tốc độ biến dạng và vận tốc va đập. Kết quả so sánh tốt về mômen uốn động tới hạn giữa phương pháp phần tử hữu hạn, phương pháp dự đoán bằng công thức thực nghiệm tìm được, và kết của thực nghiệm cho thấy độ tin cậy trong cách tính toán mô men uốn tới hạn dưới điều kiện tải trọng uốn động.

Từ khoá: Hư hỏng do uốn, Kết cấu chịu va chạm, Đáp ứng phá hủy, Thép cường độ cao, Dầm hấp thụ năng lượng

[1]*Trường Đại học Bách khoa-Đại học Quốc gia thành phố Hồ Chí Minh, Việt Nam*

[2]*Viện công nghệ kỹ thuật Bandung, Indonesia*

Liên hệ

Trần Hải, Trường Đại học Bách khoa-Đại học Quốc gia thành phố Hồ Chí Minh, Việt Nam

Email: haitran@hcmut.edu.vn

Lịch sử

- Ngày nhận: 20-09-2023
- Ngày sửa đổi: 09-11-2024
- Ngày chấp nhận: 05-08-2025
- Ngày đăng: 29-09-2025

DOI :

https://doi.org/10.32508/stdjet.v8i3.1207

Check for updates

VNUHCM PRESS

Trích dẫn bài báo này: Hải T, Gunawan L, Santosa S, Jusuf A, Dirgantara T, Đình Tuân L, Văn Tạo T. **Ứng xử hỏng do uốn của kết cấu hộp thép độ cứng cao thành mỏng dưới lực va chạm tĩnh và động**. *Sci. Tech. Dev. J. - Eng. Tech.* 2025; 8(3):2612-2622.